Computational Study in Centrifugal Compressor

Irina-Carmen ANDREI[1], Gabriela STROE[*,2]

*Corresponding author
[1]INCAS – National Institute for Aerospace Research "Elie Carafoli",
B-dul Iuliu Maniu 220, Bucharest 061126, Romania,
andrei.irina@incas.ro, icandrei28178@gmail.com
[2]POLITEHNICA University of Bucharest, Faculty of Aerospace Engineering,
Gh. Polizu Street 1-7, Sector 1, Bucharest, 011061, Romania,
ing.stroe@yahoo.com*

DOI: 10.13111/2066-8201.2018.10.3.1

Received: 29 May 2018/ Accepted: 21 June 2018/ Published: September 2018

6th International Workshop on Numerical Modelling in Aerospace Sciences, NMAS 2018*,*
16 - 17 May 2018, Bucharest, Romania, (held at INCAS, B-dul Iuliu Maniu 220, sector 6)
Section 1 – Launchers propulsion technologies and simulations of rocket engines

Abstract: *The active control for centrifugal compressor systems consists in using, monitoring and managing the sensors to detect fluid disturbances, the actuators to introduce desired perturbations and a suitable controller to determine the optimal actuator actions using the sensor information. The object of an interesting centrifugal compressor design is to obtain the most air through a given diameter compressor, with a minimum number of stages while maintaining high efficiencies and aerodynamic stability over the operating range. The high efficiency of the axial compressor system decreases dramatically when used in small high-pressure applications, especially due to the large relative tip clearance. In addition, the high centrifugal force, dominating the pressure rise, results in a superior operability and the short axial length of the centrifugal compressor offers rotor-dynamic multiple advantages. These qualities allow the centrifugal compressor system to be used as the last stage of a high-pressure compressor of an aero engine as well as turbo pump assemblies used in liquid-propelled rocket engines.*

Key Words: *Aerodynamic stability, Centrifugal compressor, control system, disturbances*

1. INTRODUCTION

For all applications dedicated to aviation, the centrifugal compressor system consists either of a dual centrifugal compressor (meaning the increase in air mass flow, since the intake is on both sides), or no more than two series of centrifugal compressors connected, due to the potential amplification of loss of pressure inside the connector ducts.

The purpose of a centrifugal compressor system is to produce a distinct increase in static pressure, thus effectively increasing the static enthalpy [3-4].

From the thermo-dynamical analysis standpoint, the compressor pressure ratio is the most significant parameter, since it enables the calculation of the jet engine performances, for all the engine running regimes and for the entire flight envelope, and also the design of the centrifugal compressor.

Centrifugal compressor rotating stall is limited to low-pressure systems and high-pressure systems at partial speed. For the most commonly used centrifugal system configuration in aeronautical applications, including high-pressure systems, while functioning at design speed, it has been noticed that the rotating stall has little effect on pressure rise and flow rate, and just serves as a precursor to surge [3-4].

All types of fluid dynamic instabilities can limit the overall compressor performances and can alter the safe operation of the entire engine. Unsteady fluctuations, caused by rotating stall or surge, may lead to excessive heating of the impeller blades and to a greater compressor exit temperature. Large amplitude fluctuations can cause additional periodic loads of the blades, which result in increased operating noise levels as well as fatigue, or even fatal damage of the centrifugal compression system [3-4].

Due to the severity of these dangerous conditions, centrifugal compressors are classically designed to operate well below the peak pressure rise point [3-4].

2. ANALITICAL MODELING OF CENTRIFUGAL COMPRESSOR CONTROL

The Navier-Stokes equations describe continuum fluid flows from the first principles of thermos-dynamics. An appropriate derivation of the Navier-Stokes equations is given in the classic paper of Schlichting [2] where terms of the Navier-Stokes equations may be simplified or neglected if certain assumptions are made [5-8].

For the numerical solution of the analytical model, the viscous effects are considered; the computational domain surrounding the body geometry is divided into small cells. Following the integration of the Navier-Stokes equations across each computational cell, the flow field at time level is completely solved [9-14]. The reason of this numerical algorithm is to advance the solution to a new time level, by using a discrete time step [9-14].

$$\delta_t \cdot \vec{q} + \delta_x \cdot \vec{E} + \delta_y \cdot \vec{F} + \delta_z \cdot \vec{G} = \delta_x \cdot \vec{R} + \delta_y \cdot \vec{S} + \delta_z \cdot \vec{T} \tag{1}$$

$$\vec{q} = \begin{bmatrix} \rho \\ \rho u \\ \rho v \\ \rho w \\ e \end{bmatrix}, \vec{E} = \begin{bmatrix} \rho u \\ \rho u^2 + p \\ \rho uv \\ \rho uw \\ (e+p)u \end{bmatrix}, \vec{F} = \begin{bmatrix} \rho v \\ \rho vu \\ \rho v^2 + p \\ \rho vw \\ (e+p)v \end{bmatrix}, \vec{G} = \begin{bmatrix} \rho v \\ \rho vu \\ \rho wv \\ \rho w^2 + p \\ (e+p)w \end{bmatrix} \tag{2}$$

$$\vec{R} = \begin{bmatrix} 0 \\ \tau_{xx} \\ \tau_{xy} \\ \tau_{xz} \\ u\tau_{xx} + v\tau_{xy} + w\tau_{xz} - q_z \end{bmatrix}, \vec{S} = \begin{bmatrix} 0 \\ \tau_{yx} \\ \tau_{yy} \\ \tau_{yz} \\ u\tau_{yx} + v\tau_{yy} + w\tau_{yz} - q_z \end{bmatrix}, \vec{T} = \begin{bmatrix} 0 \\ \tau_{zx} \\ \tau_{zy} \\ \tau_{zz} \\ u\tau_{zx} + v\tau_{zy} + w\tau_{zz} - q_z \end{bmatrix} \tag{3}$$

$$\tau_{ij} = \mu\left(\frac{\partial u_i}{\partial x_j} + \frac{\partial u_j}{\partial x_i}\right) - \frac{2}{3}\mu\frac{\partial u_k}{\partial x_k}\delta_{ij}, \quad i,j,k = 1,2,3 \tag{4}$$

$$q_i = -k\frac{\partial T}{\partial x_i}, \quad i = 1,2,3 \tag{5}$$

$$p = (\gamma - 1)\left[e - \frac{1}{2}\rho(u^2 + v^2 + w^2)\right] \tag{6}$$

$$e = c_v T \qquad h = c_p T \tag{7}$$

$$\frac{\partial}{\partial t}\iiint_V \vec{q}\,dV + \iint_S \left[\vec{E} + \vec{F} + \vec{F}\right]\cdot\vec{n}\,dS = \iint_S \left[\vec{R} + \vec{S} + \vec{T}\right]\cdot\vec{n}\,dS \tag{8}$$

$$\begin{aligned}&\iint_S \left[\vec{E} + \vec{F} + \vec{G}\right]\cdot\vec{n}\,dS \\ &\approx \left[\left(\vec{E}\cdot\vec{n}\right)|\Delta S|\right]_{i+\frac{1}{2}} + \left[\left(\vec{E}\cdot\vec{n}\right)|\Delta S|\right]_{i-\frac{1}{2}} + \left[\left(\vec{F}\cdot\vec{n}\right)|\Delta S|\right]_{j+\frac{1}{2}} \\ &+ \left[\left(\vec{F}\cdot\vec{n}\right)|\Delta S|\right]_{j-\frac{1}{2}} + \left[\left(\vec{G}\cdot\vec{n}\right)|\Delta S|\right]_{k+\frac{1}{2}} + \left[\left(\vec{G}\cdot\vec{n}\right)|\Delta S|\right]_{k-\frac{1}{2}}\end{aligned} \tag{9}$$

$$\begin{aligned}&\left(\vec{E}\cdot\vec{n}\right)|\Delta S| \approx \hat{E} \\ &\left[\left(\vec{E}\cdot\vec{n}\right)|\Delta S|\right]_{i+\frac{1}{2}} + \left[\left(\vec{E}\cdot\vec{n}\right)|\Delta S|\right]_{i-\frac{1}{2}} \approx \hat{E}_{i+\frac{1}{2}} - \hat{E}_{i-\frac{1}{2}}\end{aligned} \tag{10}$$

$$\hat{E}_{i+\frac{1}{2}} = 0.5\left\{\hat{E}_R(\vec{q}_R) + \hat{E}_L(\vec{q}_L)\right\}|_{i+1/2} - \left|\tilde{A}\right|\{\vec{q}_R - \vec{q}_L\}|_{i+1/2} \tag{11}$$

$$\vec{q}_R = \left[\rho_R, u_R, v_R, w_R, p_R\right]^T \tag{12}$$

$$\vec{q}_L = \left[\rho_L, u_L, v_L, w_L, p_L\right]^T \tag{13}$$

$$\vec{q}_R = \vec{q}_{i+1} - \frac{1}{6}\Phi^-_{i+\frac{3}{2}}(\vec{q}_{i+2} - \vec{q}_{i+1}) - \frac{1}{3}\Phi^+_{i+\frac{1}{2}}(\vec{q}_{i+1} - \vec{q}_i) \tag{14}$$

$$\vec{q}_L = \vec{q}_i + \frac{1}{3}\Phi^-_{i+\frac{1}{2}}(\vec{q}_{i+1} - \vec{q}_i) + \frac{1}{6}\Phi^+_{i-\frac{1}{2}}(\vec{q}_i - \vec{q}_{i-1}) \tag{15}$$

$$\Phi^-_{i+\frac{1}{2}} = \Phi\left(r^-_{i+\frac{1}{2}}\right), \Phi^+_{i-\frac{1}{2}} = \Phi(r^+_{i-\frac{1}{2}}) \tag{16}$$

$$r^-_{i+\frac{1}{2}} = \frac{q_i - q_{i-1}}{q_{i+1} - q_i}, r^+_{i-\frac{1}{2}} = \frac{q_{i+1} - q_i}{q_i - q_{i-1}} \tag{17}$$

$$\Phi(r) = max[0, \min(2r, 1), \min(r, 2)] \tag{18}$$

$$\hat{E}_R(\vec{q}_R) = \begin{bmatrix}\rho_R U_R \\ \rho_R U_R u_R + p_R n_x \\ \rho_R U_R v_R + p_R n_y \\ \rho_R U_R w_R + p_R n_z \\ \rho_R U_R h_{oR} - p_R n_t\end{bmatrix}, \hat{E}_L(\vec{q}_L) = \begin{bmatrix}\rho_L U_L \\ \rho_L U_L u_L + p_L n_x \\ \rho_L U_L v_L + p_L n_y \\ \rho_L U_L w_L + p_L n_z \\ \rho_L U_L h_{oL} - p_L n_t\end{bmatrix} \tag{19}$$

$$U = (\vec{V} - \vec{V}_{grid}) \cdot \vec{n}|\Delta S| \tag{20}$$

$$h_o = \frac{e+p}{\rho} \tag{21}$$

$$n_t = -(\vec{V}_{grid} \cdot \vec{n})|\Delta S| \tag{22}$$

$$\left|\tilde{A}\right|\{\vec{q}_R - \vec{q}_L\}|_{i+1/2} = \Delta\vec{q} = \left|\tilde{\lambda}_1\right|\Delta\vec{q} + \delta_1\widetilde{U}^* + \delta_2\widetilde{N}_n \tag{23}$$

$$\widetilde{U}^* = \begin{bmatrix} \tilde{q} \\ \tilde{q}\tilde{u} \\ \tilde{q}\tilde{v} \\ \tilde{q}\tilde{w} \\ \tilde{q}\tilde{h}_o \end{bmatrix}, \widetilde{N}_n = \begin{bmatrix} 0 \\ n_x \\ n_y \\ n_z \\ \widetilde{U} \end{bmatrix} \tag{24}$$

$$\delta_1 = \left(-\left|\tilde{\lambda}_1\right| + \frac{\left|\tilde{\lambda}_2\right| + \left|\tilde{\lambda}_3\right|}{2}\right)\frac{\Delta p}{\tilde{q}\tilde{a}^2} + \frac{\left|\tilde{\lambda}_2\right| - \left|\tilde{\lambda}_3\right|}{2}\frac{\Delta U}{\tilde{a}} \tag{25}$$

$$\delta_2 = \left(-\left|\tilde{\lambda}_1\right| + \frac{\left|\tilde{\lambda}_2\right| + \left|\tilde{\lambda}_3\right|}{2}\right)\tilde{\rho}\Delta U + \frac{\left|\tilde{\lambda}_2\right| - \left|\tilde{\lambda}_3\right|}{2}\frac{\Delta p}{\tilde{a}} \tag{26}$$

$$\tilde{\lambda}_1 = \widetilde{U}, \tilde{\lambda}_2 = \widetilde{U} + \tilde{a}, \tilde{\lambda}_3 = \widetilde{U} - \tilde{a} \tag{27}$$

$$\tilde{q} = \sqrt{\rho_R\rho_L} \tag{28}$$

$$\widetilde{\Phi} = \Phi_L\left(\frac{1}{1+\sqrt{\rho_R\rho_L}}\right) + \Phi_R\left(\frac{\sqrt{\rho_R\rho_L}}{1+\sqrt{\rho_R\rho_L}}\right) \tag{29}$$

$$\frac{\Delta\hat{q}^n}{\Delta t} = \hat{E}^{n+1}_{i+1/2} - \hat{E}^{n+1}_{i-\frac{1}{2}} + \hat{F}^{n+1}_{j+\frac{1}{2}} - \hat{F}^{n+1}_{j-\frac{1}{2}} + \hat{G}^{n+1}_{k+\frac{1}{2}} - \hat{G}^{n+1}_{k-1/2} \tag{30}$$

$$\Delta\hat{q}^n = (\hat{q}^{n+1} - \hat{q}^n)\Delta V \tag{31}$$

$$\hat{E}^{n+1} = \hat{E}^n + \hat{A}^n\Delta\hat{q}^n \tag{32}$$

$$\hat{F}^{n+1} = \hat{F}^n + \hat{B}^n\Delta\hat{q}^n \tag{33}$$

$$\hat{G}^{n+1} = \hat{G}^n + \hat{C}^n\Delta\hat{q}^n \tag{34}$$

$$\hat{A}^n = \left[\frac{\partial\hat{E}}{\partial\hat{q}}\right]^n, \quad \hat{B}^n = \left[\frac{\partial\hat{F}}{\partial\hat{q}}\right]^n, \quad \hat{C}^n = \left[\frac{\partial\hat{G}}{\partial\hat{q}}\right]^n \tag{35}$$

$$M^n\Delta\hat{q}^n = -\Delta t R^n \tag{36}$$

$$R^n = \begin{bmatrix} \hat{E}^n_{i+1/2} & -\hat{E}^n_{i-1/2} & +\hat{F}^n_{j+1/2} & -\hat{F}^n_{j-1/2} & +\hat{G}^n_{k+1/2} & -\hat{G}^n_{k-1/2} \end{bmatrix} \tag{37}$$

$$M^n \approx M_1^n M_2^n M_3^n \tag{38}$$

$$M_1^n = \begin{bmatrix} \ddots & \ddots & \ddots & \ddots & \\ & -\Delta t\hat{A}_{i-1/2}^n & I & \Delta t\hat{A}_{i+1/2}^n & \\ & \ddots & \ddots & \ddots & \ddots \end{bmatrix} \tag{39}$$

$$M_1^n \Delta\hat{q}^* = -\Delta t R^n \tag{40}$$

$$M_2^n \Delta\hat{q}^{**} = \Delta q^n \tag{41}$$

$$M_{13}^n \Delta\hat{q}^* = \Delta\hat{q}^{**} \tag{42}$$

$$\hat{A}_i^n = (T\hat{\Lambda}T^{-1})_i \tag{43}$$

$$-\left(T\hat{\Lambda}T^{-1}\right)_i \Delta\hat{q}_{i-1}^* + I\Delta\hat{q}_i^* + \left(T\hat{\Lambda}T^{-1}\right)_i \Delta\hat{q}_{i+1}^* = -\Delta t R^n \tag{44}$$

$$-\hat{\Lambda}_i(T^{-1}\Delta\hat{q}_{i-1}^*) + I(T^{-1}\Delta\hat{q}_i^*) + \hat{\Lambda}_i(T^{-1}\Delta\hat{q}_{i+1}^*) = -\Delta t T^{-1} R^n \tag{45}$$

$$-\overline{u_i' u_j'} = v_t\left(\frac{du_i}{dx_j} + \frac{du_j}{dx_i}\right) \tag{46}$$

$$v_t = \tilde{v} f_{v1},\ \ f_{v1} = 1 - \frac{\chi^3}{\chi^3 + c_{v1}^3},\ \ \chi = \frac{\tilde{v}}{v} \tag{47}$$

$$\tilde{S} = S + \frac{\tilde{v}}{\kappa^2 d^2} f_{v2},\ \ f_{v2} = 1 - \frac{\chi}{1 + \chi f_{v1}} \tag{48}$$

$$f_w = g\left[\frac{1 + c_{w3}^6}{g^6 + c_{w3}^6}\right]^{1/6},\ \ g = r + c_{w3}(r^6 - r),\ \ r = \frac{\tilde{v}}{\tilde{S}\kappa^2 d^2} \tag{49}$$

$$f_{t1} = c_{t1} g_t \exp\left(-c_{t2}\frac{w_t^2}{\Delta U^2}(d^2 + g_t^2 d_t^2)\right) \tag{50}$$

$$f_{t2} = c_{t3}\exp(-c_{t4}\chi^2) \tag{51}$$

$$g_t = \min\left(0.1, \frac{\Delta U}{w_t}\Delta x_t\right) \tag{52}$$

$$\frac{p_n}{\sqrt{\zeta_x^2 + \zeta_y^2 + \zeta_z^2}} = \rho\left(\frac{\partial\zeta_t}{\partial\tau} + u\frac{\partial\zeta_x}{\partial\tau} + v\frac{\partial\zeta_y}{\partial\tau} + w\frac{\partial\zeta_z}{\partial\tau}\right) \tag{53}$$

$$\frac{\partial}{\partial t}\left(\frac{2a}{\gamma - 1} - u_n\right) + (u - a)\frac{\partial}{\partial n}\left(\frac{2a}{\gamma - 1} - u_n\right) = 0 \tag{54}$$

$$\left.\frac{2a}{\gamma - 1} - u_n\right|_{i=1} = \left.\frac{2a}{\gamma - 1} - u_n\right|_{i=2} \tag{55}$$

$$\frac{a^2}{\gamma - 1} + \frac{u_n^2}{2} = c_p T_0 \tag{56}$$

$$\frac{\partial}{\partial t}(\rho_p V_p) = \dot{m}_c - \dot{m}_t \tag{57}$$

$$V_p \frac{\partial \rho_p}{\partial p_p}\frac{\partial p_p}{\partial t} = \dot{m}_c - \dot{m}_t \tag{58}$$

$$a_p^2 = \frac{\partial p_p}{\partial \rho_p} \tag{59}$$

$$\frac{\partial p_p}{\partial t} = \frac{a_p^2}{V_p}(\dot{m}_c - \dot{m}_t) \tag{60}$$

$$p_p^{n+1} = p_p^n + C(\dot{m}_c - \dot{m}_t)\Delta t \tag{61}$$

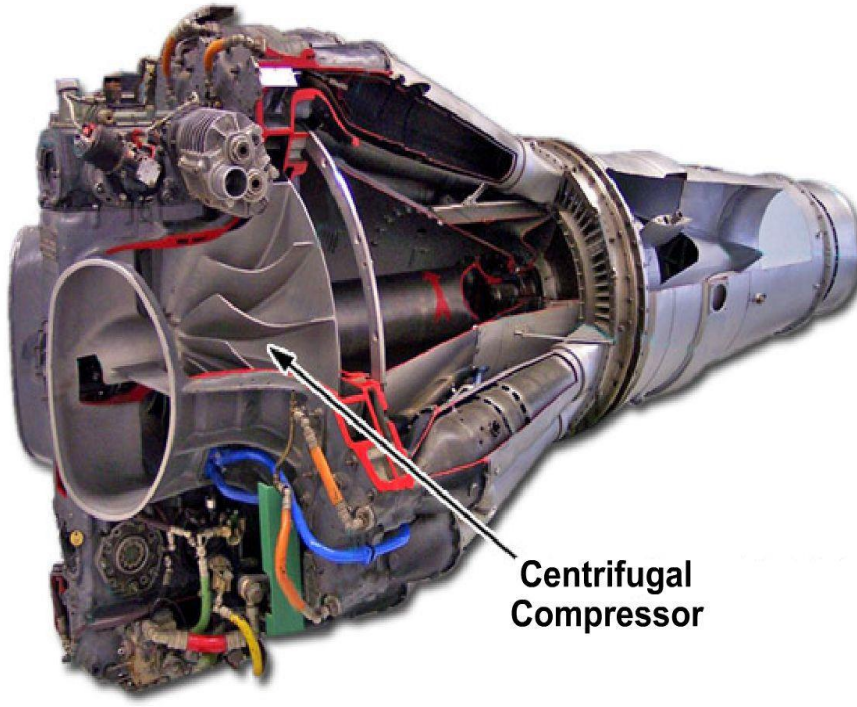

Fig. 1 - Centrifugal compressor assembly for a turbojet engine [1]

The safety margin of 10 to 20 percent is generally introduced between the surge line and the design compressor system operating conditions [15-17].

In the last years, due to the implementation of appropriate stall detection and stall avoidance devices, the safety margin has been significantly reduced [18-20].

The implementation of such precuation measures enable the safe operation of the centrifugal compressor, especially for the operating conditions: higher pressure ratios and smaller flow rates [18-20].

Following a large survey on this topic, the control of the centrifugal compressor operation falls into one of these two categories:

(1) passive or open-loop control, and

(2) active or closed-loop control.

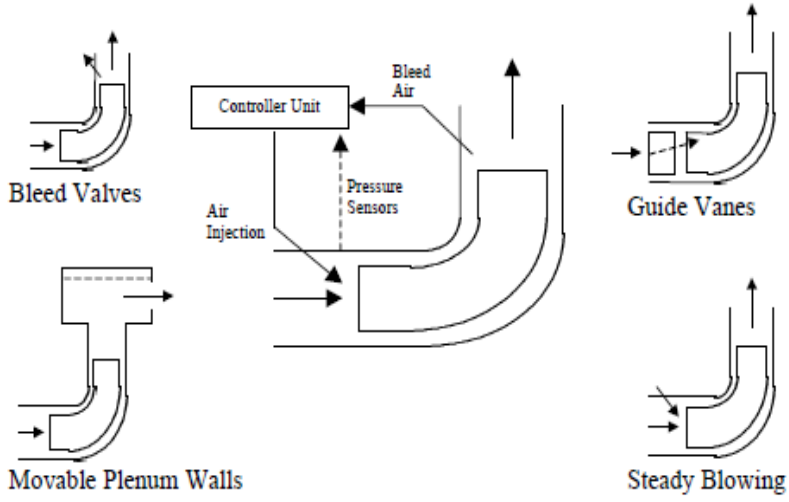

Fig. 2 - Active & passive control for the centrifugal compressor, intended as a part of a jet engine

Open-loop control is reached following changes induced in the centrifugal compressor design and construction such that the performance characteristic map is modified and the surge line is shifted to smaller flow rates [18-20]. Open-loop control methods are aimed to moving the pressure peak to smaller mass flow rates, even taking all risks supposed by slight decrease in adiabatic efficiency. The active control method is used via a direct link between the controller unit and a set of actuation devices [18-20]. Pinsley et all [21] presented a plenum gate valve to control the flow leaving the compression system. The valve was operated at frequencies tailored to damp out all potential disturbances that would lead to the onset of surge. The closed-loop control in centrifugal compressor is an ongoing area of research with advancements, which can bring significant improvements in centrifugal compressor performance; certain issues that are real challenges, require a proper solution and construction, prior to be applied in closed-loop compressor control in engines [21]. The high pressure ratio as well as the superior operability characteristics of the centrifugal compressor make it suitable as a compressor system part of an aero engine [22]. The continuous increase of the pressure ratios, intended as a main jet engine design parameter, as well as the increase in air traffic and the growing number of restrictions with respect to fuel consumption in conjunction with the environmental restrictions for emissions, require a better understanding of the detailed aerodynamics of the centrifugal compressor [22]. Especially in the coming future, new aerodinamical propulsion concepts with intercooled compressors using a centrifugal compressor as an intermediate stage between the low and the high-pressure compressor system will create a high and strong potential for new generations of centrifugal compressors. The use of the centrifugal compressors as parts of the aero engines is in a certain extent restricted by the pressure ratio, i.e. for values larger than 6, local inclusions of supersonic flow within the impeller can occur and further develop, with the consequent manifest of the intense pressure losses, due to presence of shock waves. This is why centrifugal compressors are not widely used for all aero engines but, on the other hand, the flow inside a centrifugal compressor is very intricate, with three-dimensional complex intrinsic features; therefore, the level of know-how regarding the detailed aerodynamics of this type of compressor as part of jet engines, needs an in-depth study, far much rich in details than the axial compressor [22].

3. NUMERICAL SIMULATION AND CONCLUSIONS

Advancements in numerical simultion methods and experimental studies are providing new insights into the aerodynamics of the centrifugal compressor and are being applied to increase the compressor's efficiency as well as the operating range. The challenge of the centrifugal compressor remains the design of the diffusion system.

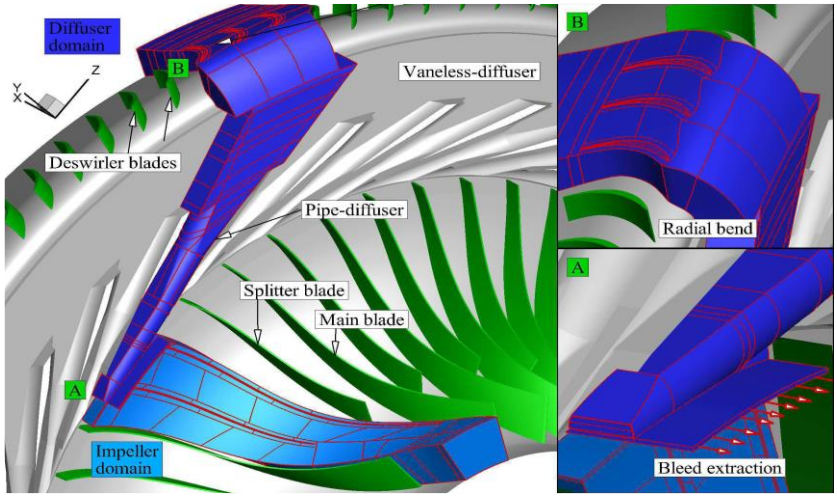

Fig. 3 - Schematic diagram of a centrifugal compressor, highlighting the 3D computational domain for the impeller [22]

The Computational Fluid Dynamics CFD simulations carried on for the steady-state represent an essential instrument in the design process of centrifugal compressors systems.

The design of centrifugal compressors involves the use of computational methods in conjunction with experimental validation to provide precise analysis with a fast turn-around between design iterations. The difficulty that appears when using computational methods is the simulation turn over time, which depends heavily on the grid used, boundary conditions applied (meaning a proper selection of types of boundary layer conditions and most adequate and case tailored distribution of parameter values on the boundaries, both equally important) and the turbulence model chosen. Full stage unsteady numerical simulations are usually too expensive and time consuming for the iterative design process, but in certain cases, requiring high IT system performances, the full stage unsteady numerical simulations can be used for animations and preparations for complex multidisciplinary laboratories, such as the 3D Virtual Laboratory, enabling complex studies on this topic. Steady-state models which use a mixing plane method to model the interface between rotating and stationary domains are favorite due to the considerably reduced simulation time. However, the importance of turbulence model chosen still plays a significant role in obtaing realistic predictions of the centrifugal compressor performance. The turbulence models in current use, which consist in a single equation or a set of non-linear partial differential equations, must be associated to the Navier-Stokes equations, in purpose to completely describe the complex features of the flow, including the effects of viscosity and turbulence. It is very useful to integrate certain Preparatory Tools in a CFD code, with the intent of computing time reducing. In case of the centrifugal compressor, for both design process and off-design operational performance analysis, the use of and date management from the Universal Map is compulsorily and very important. The coordinates of the Universal map are the corrected flow (62) versus the pressure ratio (63):

$$Corrected\_flow = \dot{M}_a \frac{\sqrt{T_1^*}}{p_1^*} \tag{62}$$

$$Pressure\_ratio = \pi_c^* = \frac{p_2^*}{p_1^*} \tag{63}$$

$$Speed_{regime} = nbar = \bar{n} = \frac{n_{off-design}}{n_{design}} \tag{64}$$

As one can easily notice, the surge line is highlighted (in red contour). Speed operation regime lines reflect the behavior of the centrifugal compressor at off-design regimes, from idle (50%), up to cruise (95%), design (100%) and maximum (105%). The centrifugal compressor efficiency domain ranges from 0.65 up to 0.78, the constant efficiency contours being well represented within the Universal Map field.

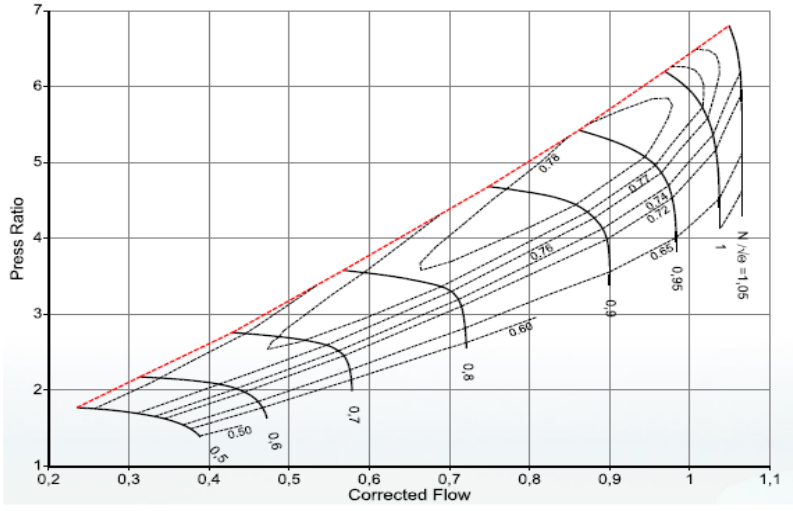

Fig. 4 – Universal Map of a centrifugal compressor, where design pressure ratio = 5.9, [23]

A useful Preparatory Tool was designed following a thorough study with regard to the construction of the approximation functions for the constant speed regime lines. The difficulty of such approach, is given by the fact that if the cartesian reference system is considered as corrected flow versus pressure ratio, large errors on pressure ratio will be introduced for small variation s of the corrected flow, which aspect becomes more evident with the increase of the speed regime, e.g. over 80%. A more efficient approach, which also expels this inconvenient, consists in shifting the coordinates of the cartesian reference system.

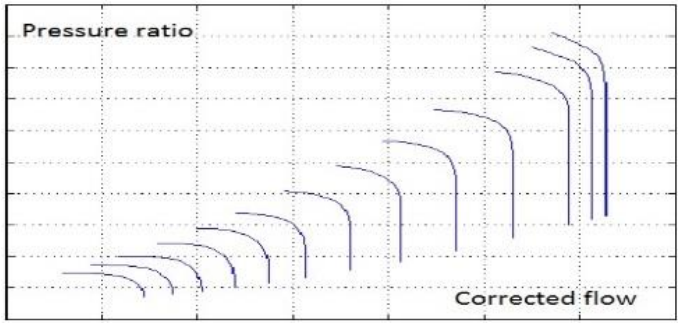

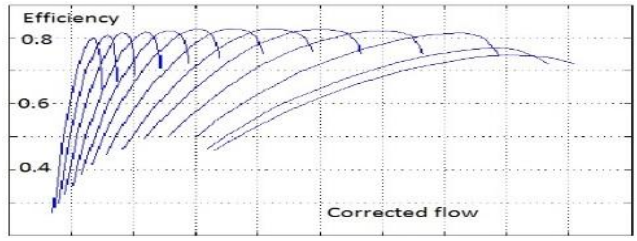

Fig. 5 – Universal Compressor Map, expressed as
Pressure ratio and efficiency versus corrected flow

Different study cases were investigated to obtain an optimal design of the centrifugal compressor, and further, to design the proper control system.

Numerical simulations have been performed for the turbojet engine thrust control. The variations of the specific thrust [Ns/kg] of the turbojet engine versus the speed regime (64), for different nozzle exit areas A5 [m^2] are illustrated in the next diagrams.

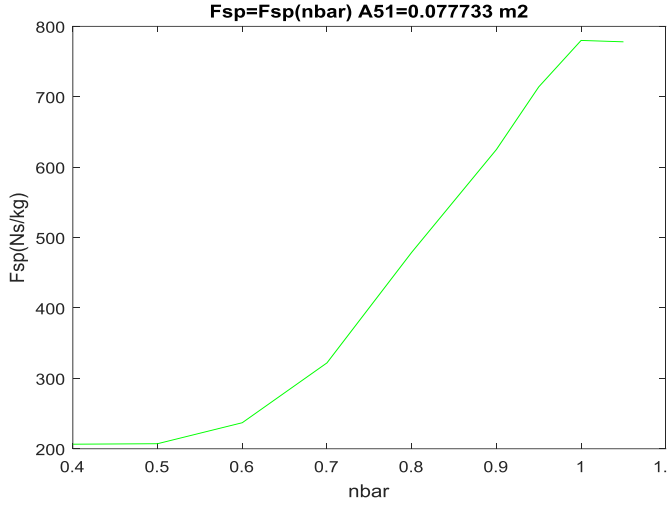

Fig. 6.1 – Numerical simulations for turbojet engine thrust control

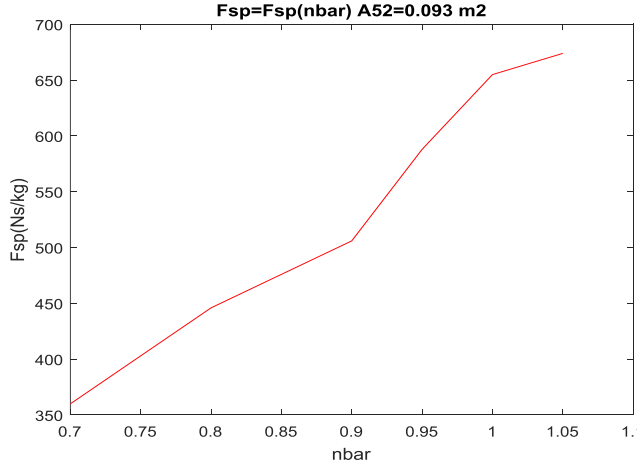

Fig. 6.2 – Numerical simulations for turbojet engine thrust control

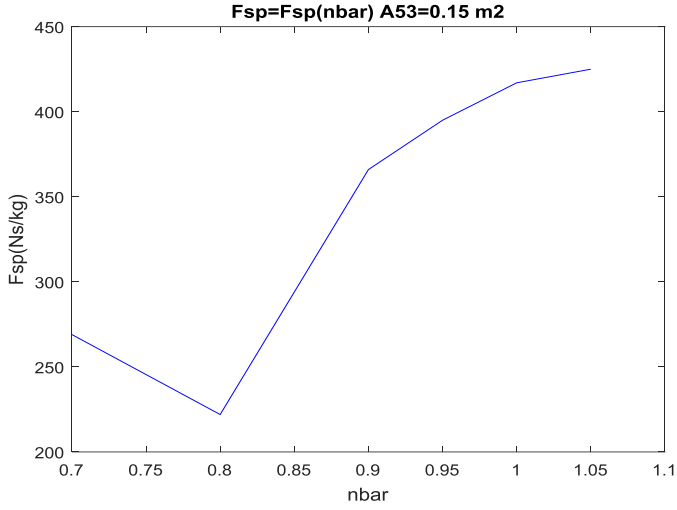

Fig. 6.3 – Numerical simulations for turbojet engine thrust control

The control system is designed such that to take advantage for the time allowance and to use slower-responding control elements, and eventually to provide a temperature regulation.

Fuel flow is selected as the rotor speed limiting element, although fuel flow can be used for both temperature and rotor speed regulation, on simple aero engines.

Over-temperature condition for very short periods, required by engine acceleration or other transients, can also be accepted.

REFERENCES

[1] * * * http://navybmr.com/study%20material/14008a/14008A_ch1.pdf
[2] H. Schlichting, *Boundary Layer Theory*, Seventh Edition, McGraw-Hill, New York, 1979.
[3] P. B. Lawless, S. Fleeter, Active Control of Rotating Stall in a Low-Speed Centrifugal Compressor, *J. Propulsion and Power*, Vol. **15**, No. 1, pp. 38-44, January-February 1999.
[4] B. Jager, *Rotating Stall and Surge Control*, Proceedings of the 34th Conference on Decision & Control, New Orleans, LA., 1995.
[5]* * * http://math.mit.edu/~gs/cse/codes/mit18086_navierstokes.pdf.
[6] A. J. Chorin, J. E. Marsden, *A mathematical introduction to fluid mechanics*, Third edition, Springer, 2000.
[7] G. Strang, *Computational Science and Engineering*, First Edition, Wellesley-Cambridge Press, 2007.
[8] * * * http://web.cecs.pdx.edu/~gerry/class/ME448/notes/pdf/convectionUpwind.pdf.
[9] J. D. Mattingly, *Elements of gas turbine propulsion*, Sixth reprint, 2013. https://soaneemrana.org/onewebmedia/ELEMENTS%20OF%20GAS%20TURBINE%20PROPULTION 2.pdf
[10] D. A. Anderson, J. C. Tannehill, R. H. Pletcher, *Computational Fluid Mechanics and Heat Transfer*, 2nd Ed., McGraw-Hill, New York, 1997.
[11] C. Hirsch, *Numerical Computation of Internal and External Flows*, Vol. **I** & **II**, 1st Ed., Wiley, New York, 1988.
[12] P. L. Roe, *Some Contributions to the Modeling of Discontinuous Flows*, Large-Scale Computations in Fluid Mechanics, Edited by B.E. Engquist, S. Osher, R.C.J. Somerville, Vol. **22**, Part.2, Lectures in Applied Mathematics, ASME, Providence.
[13] Y. Liu, M. Vinokur, *Upwind Algorithms for General Thermo-Chemical Nonequilibrium Flows*, AIAA Paper, 89-0201.
[14] H. P. Pulliam, J. L. Steger, Implicit Finite-Difference Simulations of Three-Dimensional Compressible Flow, *AIAA Journal*, Vol. **18**, No. 2, February 1980.
[15] P. R. Spalart, S. R. Allmaras, *A One-Equation Turbulence Model for Aerodynamic Flows*, AIAA Paper 92-0439

[16] P. G. Hill, C. R. Peterson, *Mechanics and Thermodynamics of Propulsion*, 2nd Ed., Addison Wesley Publication Co., 1992.
[17] A. S. Ucer, P. Stow, C. Hirsch, *Thermodynamics and Fluid Mechanics of Turbomachinery*, 1985.
[18] J. T. Gravdahl, O. Egeland, *Compressor Surge and Rotating Stall Modeling and Control*, Springer, 1999.
[19] Y. Ochi, Flight Control System Design for Propulsion-Controlled Aircraft, Proceedings of the Institute of Mechanical Engineering Part G - *Journal of Aerospace Engineering*, 2005.
[20] M. Harefors, D. G. Bates, Integrated Propulsion-based Flight Control System Design for a Civil Transport Aircraft, *International Journal of Turbo and Jet Engines*, Vol. **20**, No. 2, 2003.
[21] J. E. Pinsley, G. R. Guenette, A. H. Epstein, E. M. Greitzer, Active Stabilization of Centrifugal Compressor Surge, *J. Turbomachinery*, Vol. **113**(4), 723-732, Oct 01, 1991.
[22] * * * https://core.ac.uk/download/pdf/36622858.pdf.gas
[23] J. Kurzke, Compressor and Turbine maps for Gas Turbine Performance Computer Programs, Issue 3, *Gas Turb GmbH*, 2013.